International Journal of QUANTUM CHEMISTRY

The Effects of Resonance Delocalization and the Extent of π System on Ionization Energies of Model Fluorescent Proteins Chromophores

Julia Lazzari-Dean,[a] Anna I. Krylov,[a] and Ksenia B. Bravaya*[b]

Recent advances in the design and application of redox-active fluorescent proteins (FPs) stimulated an interest in the electronic structure of the ionized/electron-detached FP chromophores. Here, we report the results of a computational study of the electron-detached and ionized states of model chromophores of green and red FPs. We focus on the analysis of the effects of the phenolate OH group position (ortho, meta, and para) on relative energies of the chromophores in the ground as well as in the ionized/detached electronic states. We found that, similarly to the green chromophore, the red chromophores with the OH group in meta position have lower vertical detachment energies (DE) and greater ionization energies relative to the ortho and para forms. Moreover, the effect is stronger for the red anionic chromophores. The differences in DE in meta species relative to their para counterparts are 0.47 and 0.25 eV for the red and green chromophores, respectively. The observed trends are due to a combined effect of resonance stabilization and the electronegativity of the acylimine group in the red chromophores. The analysis is supported by the computed charge and spin density delocalization patterns. © 2014 Wiley Periodicals, Inc.

DOI: 10.1002/qua.24825

Introduction

Redox processes are of paramount importance in chemistry, biology, and materials science (e.g., photovoltaics and molecular electronics). Electron ejection from and attachment to a molecule can be initiated by various mechanisms, for example, electrochemically, through an electrode to absorbed species, by electron transfer to/from another molecule, or induced by photon absorption. The latter process is the basis of various photoelectron spectroscopies that enable probing molecular structure and wave functions. Photoinduced electron transfer is the key step in a number of biological processes including photosynthesis,[1,2] DNA radiation damage repair by photolyases,[3] photoconversions in fluorescent proteins (FPs),[4] and more. The first step toward the understanding and quantitative description of photoinduced electron transfer events entails accurate characterization of the oxidized/reduced states involved.

The quantities that govern the oxidation energetics are ionization energies (IE) or detachment energies (DE), corresponding to electron ejection from neutrals or anions, respectively. Thus, understanding the relationship between molecular structures and IEs/DEs is a prerequisite for prediction and control of the redox properties of molecules in more complex environments, such as solvents and proteins. Recent photodetachment and action spectroscopy experiments[5–9] have significantly improved our understanding of the photoinduced processes in isolated GFP chromophores, including competing photodetachment and radiationless relaxation channels. However, less is known on the photophysics of the isolated red chromophores.

Motivated by potential bioimaging applications[10,11] and, in particular, photoinduced redox activity of FPs,[12,13] we have been investigating the electron donating/accepting ability of model and protein-bound chromophores.[14–20] These chromophores feature extensive π-conjugated systems; two examples are shown in Figure 1. Depending on the conditions, the chromophores exist in either neutral (protonated on the phenolic end) or anionic (deprotonated, phenolate-like) forms. 4-hydroxybenzylidene-1,2-dimethylimidazolinone (HBDI), which consists of the phenol and imidazolinone moieties connected by a methine bridge, is a model for the chromophores of wild-type green fluorescent protein (wt-GFP) and several important mutants (e.g., EGFP). 4-hydroxybenzylidene-1-methyl-2-penta-1,4-dien-1-yl-imidazolin-5-one (HBMPDI) has a similar structure but its π-system is extended by an acylimine moiety. This more extended conjugation leads to a red-shifted absorption; such chromophores are found in several red FPs.[11]

In this article, we compare the effects of the OH group position (ortho, meta, and para) and the elongation of the π-conjugated chain (HBDI versus HBMPDI) on the electron detachment from the chromophores in the neutral and anionic forms (see Fig. 1). In our previous work,[16,17] we investigated redox properties of model GFP chromophores (ortho, para, and meta HBDI, as well as their methylated analogues) and also compared p-HBDI with model red (HBMPDI) and blue

[a] *J. Lazzari-Dean, A. I. Krylov*
Department of Chemistry, University of Southern California, Los Angeles, California 90089-0482
[b] *K. B. Bravaya*
Department of Chemistry, Boston University, Boston, Massachusetts 02215
E-mail: kbravaya@gmail.com

Contract grant sponsor: U.S. National Science Foundation (A.I.K.); contract grant number: CHE-1264018.

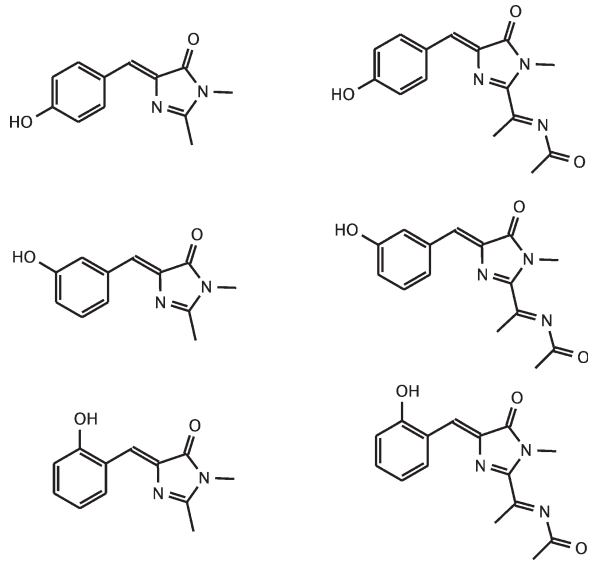

Figure 1. Chemical structures of the para- (top), meta- (middle), and ortho- (bottom) isomers of HBDI (left) and HBMPDI (right). Substitutions in positions 2, 3, and 4 in the phenolate ring have been considered.

chromophores. We found that these structural modifications have a noticeable effect on IEs/DEs and, consequently, redox potentials. The main difference between the ortho, meta, and para HBDI structures is due to resonance conjugation (which is shut down in the meta isomer) that affects orbital delocalization[16,17,21] (Fig. 2). Interestingly, the trends in the neutral and anionic species were different; this has been explained by a greater effect that resonance has on charged species.[17] This study investigates whether this effect holds in red chromophores and whether resonance interactions are affected by the presence of the acylimine tail. We also analyze the patterns of the unpaired spin and charge localization.

The acylimine moiety is believed to participate in π-conjugation, giving rise to a red-shifted absorption.[11] However, its effect on redox properties and, especially, charge/spin delocalization is less obvious. Here, we investigate whether delocalization into the acylimine tail of HBMPDI mitigates or enhances the effect of ortho/meta/para structural variations.

There are different ways to characterize electronic structure of the ionized states. The difference between the initial N and target N–1 electron states can be quantified by the Dyson orbital[22]:

$$\phi^d(1) = \sqrt{N}\int \Psi_i(N)\Psi_f(N-1)d2\ldots dN \qquad (1)$$

Dyson orbitals (which are related to experimental observables such as cross sections)[23] show exactly what was carved out by ionization and from where the negative charge and spin were removed. When using a Hartree–Fock (HF) wave function as $\Psi_i(N)$ in Eq. (1) and an unrelaxed Slater determinant as $\Psi_f(N-1)$, the Dyson orbital is just a molecular orbital from which the electron is removed, as one would expect based on Koopmans' picture of ionization. Positive charge and unpaired spin density distributions in the target ionized state coincide with the square of the Dyson orbital only in the case of Koopmans' description. If one includes correlation and/or orbital relaxation effects, the distribution will change even if nuclei remain at the same positions as in the initial state. This difference can be observed even when using mean-field wave functions if one uses relaxed orbitals to represent Ψ_f. For example, for the radical states that have an excess α-electron, the spin density has both α and β parts; pure α unpaired density is only obtained within Koopmans' restricted open-shell HF (ROHF) framework.

We also note that deviation from the Koopmans' picture implies that spin and charge localization in the final (ionized) state are not identical, which means that charge and unpaired spin distributions can be affected by electron correlation and orbital relaxation in different ways. This distinction can be illustrated by considering a multiconfigurational wave function of the target ionized state based on a restricted open-shell HF reference. In this case, spin-adapted configurations that do not involve a singly occupied molecular orbital (SOMO) can lead to significant deviation from the Koopmans positive charge distribution, but the unpaired spin density is still consistent with the SOMO. Thus, charge and spin densities provide complementary information on the electronic structure of the target ionized state.

This article addresses the effects of resonance and conjugated chain elongation on IEs/DEs. The effects of para, meta, and ortho position of the hydroxyl group in the phenolate moiety for the red chromophore are consistent with the previously observed trends in HBDI: greater vertical IEs (VIEs) for the neutral meta form (relative to the ortho and para forms) and the opposite trend for the anionic forms. In addition to DEs and IEs, we analyze the effect of the resonance on the structural parameters, charge and unpaired spin density distributions.

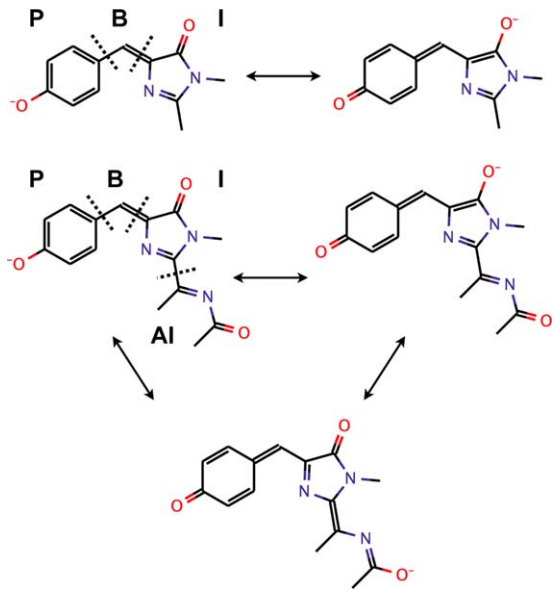

Figure 2. Dominant resonance structures of anionic p-HBDI (top) and p-HBMPDI (bottom). P, B, I, and AI denote phenolate, bridge, imidazolinone, and acylimine moieties, respectively.

Table 1. Effect of resonance conjugation on bond length alternation Δ, Å.

System	ΔCC_B	ΔCO_{PI}
p-HBDI	0.086	0.143
m-HBDI	0.089	0.146
o-HBDI	0.088	0.147
p-HBDI-D	0.016	0.015
m-HBDI-D	0.060	0.033
o-HBDI-D	0.029	0.020
p-HBMPDI	0.077	0.146
m-HBMPDI	0.083	0.146
o-HBMPDI	0.080	0.142
p-HBMPDI-D	0.014	0.015
m-HBMPDI-D	0.037	0.034
o-HBMPDI-D	0.008	0.012

Δ is defined as the difference in bond length between two bonds of the same type. ΔCO_{PI} is defined as the difference in length between the CO bonds in the phenolate and imidazolinone moieties. ΔCC_B is the difference between bond lengths of the two bridge CC bonds. Subscripts of P, I, and B denote the phenolate, imidazole, and bridge fragments, respectively.

Computational Details

Equilibrium geometries were optimized at the RI-MP2/cc-pVTZ and ωB97X-D/cc-pVTZ levels of theory.[24–26] A matching rimp2-cc-pVTZ auxiliary basis set was used in the RI-MP2 calculations.[27] All electrons were active in RI-MP2 geometry optimizations. All Cartesian geometries and relevant energies are given in Supporting Information.

Natural bond orbital (NBO) analysis[28] was performed using the ωB97X-D/cc-pVTZ densities at the ωB97X-D/cc-pVTZ optimized geometries. Unrestricted DFT was used in all calculations of open-shell species. VIE and vertical detachment energies (VDEs) were computed with ωB97X-D/cc-pVTZ using the RI-MP2/cc-pVTZ optimized structures. Validated in our previous studies of the phenolate and anionic chromophore of HBDI[19] as well as DNA bases,[29] this protocol reliably reproduces highly accurate equation-of-motion coupled-cluster for ionization potentials (EOM-IP-CCSD) results. DFT calculations were performed using an Euler–Maclaurin–Lebedev (75 and 302) grid. S^2 expectation values were carefully monitored in all unrestricted DFT calculations and were found to lie within 0.75–0.80 and 0.85–0.90 for the cationic and neutral radicals, respectively. Thus, no significant spin contamination was observed.

All calculations were performed using Q-Chem.[30,31]

Results and Discussion

To quantify the effects of the extended π-conjugated system and resonance on the electronic structure of closed-shell (anion/neutral) and ionized (neutral/cation) states we focus on three properties: (i) bond length alternation (BLA); (ii) IEs/DEs; and (iii) charge and spin density localization patterns.

Bond length alternation

Below we use the notation HBDI-D and HBMPDI-D to refer to the anionic species (deprotonated chromophores), and HBDI and HBMPDI-for the neutrals (protonated chromophores). Structural parameters of the model chromophores (see Fig. 1) are listed in Table 1. The three main factors that affect resonance delocalization and, consequently, BLA in the chromophore's π-conjugated system are: the length of the size of the π-system (HBDI vs. HBMPDI), charge state (anion vs. neutral), and position of the OH group (para, meta, and ortho forms). Note that the three effects are not necessarily additive.

We start by discussing the effects of the charge state of the chromophore on the BLA. BLA on the methine bridge is a sensitive measure of the degree of the resonance conjugation in the green and red chromophores. It is quantified by the parameter ΔCC_B, defined as the difference in length between formally single and double bridge bonds, that is, $\Delta = 0$ corresponds to perfect resonance delocalization, as in allyl. As previously discussed[14,16,21] for p-HBDI, the anionic chromophores feature a more pronounced bond-order scrambling owing to the resonance forms shown in Figure 2. Indeed, ΔCC_B values are 0.016 and 0.086 Å for p-HBDI-D and p-HBDI, respectively. In the latter, the C_BC_P and C_BC_I bonds have clear single- and double- bond character. The pattern is also observed for the meta forms (both anionic and neutral), for example, ΔCC_B of 0.089 and 0.060 Å for m-HBDI and m-HBDI-D, respectively. A similar trend is exhibited by ΔCO_{PI}, defined as the difference in length between the CO bond in the phenolate and imidazolinone fragments. The same differences in ΔCC_B are observed for HBMPDI and HBMPDI-D chromophores: the BLA decreases by 0.063 Å (para) and 0.046 Å (meta) for HBMPDI-D relative to HBMPDI.

The second factor is the position of the OH group in the phenolate ring; it has a more prominent effect in anionic chromophores because the protonated forms are characterized by a single resonance form. One can anticipate greater ΔCC_B for the anionic meta forms relative to the para and ortho ones because there is no resonance between the rings.[16] For example, ΔCC_B values are 0.060 and 0.016 Å for meta and para HBDI-D, respectively. Stronger BLA for the meta and neutral forms, relative to the ortho and para anions, is also observed in the red chromophores (HBMPDI). The ΔCC_B values are 0.037 and 0.014 Å for m-HBMPDI-D and o-HBMPDI-D, respectively.

Finally, the extension of the π-conjugated systems by acylimine moiety facilitates further charge delocalization in anions. This results in less pronounced BLA (e.g., lower ΔCC_B) for the anionic red chromophores compared to their green analogues: 0.014 versus 0.016 Å, 0.037 versus 0.083 Å, and 0.008 versus 0.029 Å for para, meta, and ortho forms, respectively. Extension of the π-conjugated system has almost no effect on the BLA in neutrals.

Conjugation may also affect the planarity of the chromophore. Whereas the phenolate and imidazolinone moieties are coplanar in all species, the acylimine tail is not in the plane due to its greater flexibility and the steric repulsion between the methyl group and imidozalinone. The deviation from planarity can be characterized by the CNCO dihedral angle (planar structure corresponds to zero angle). In all neutral species, the dihedral angle is 78°, whereas in the anionic para and ortho species it decreases to ≈ 50°. Thus, consistent with the conclusions based on bond lengths, the dihedral acylimine angle also suggests greater resonance interactions in the anionic species.

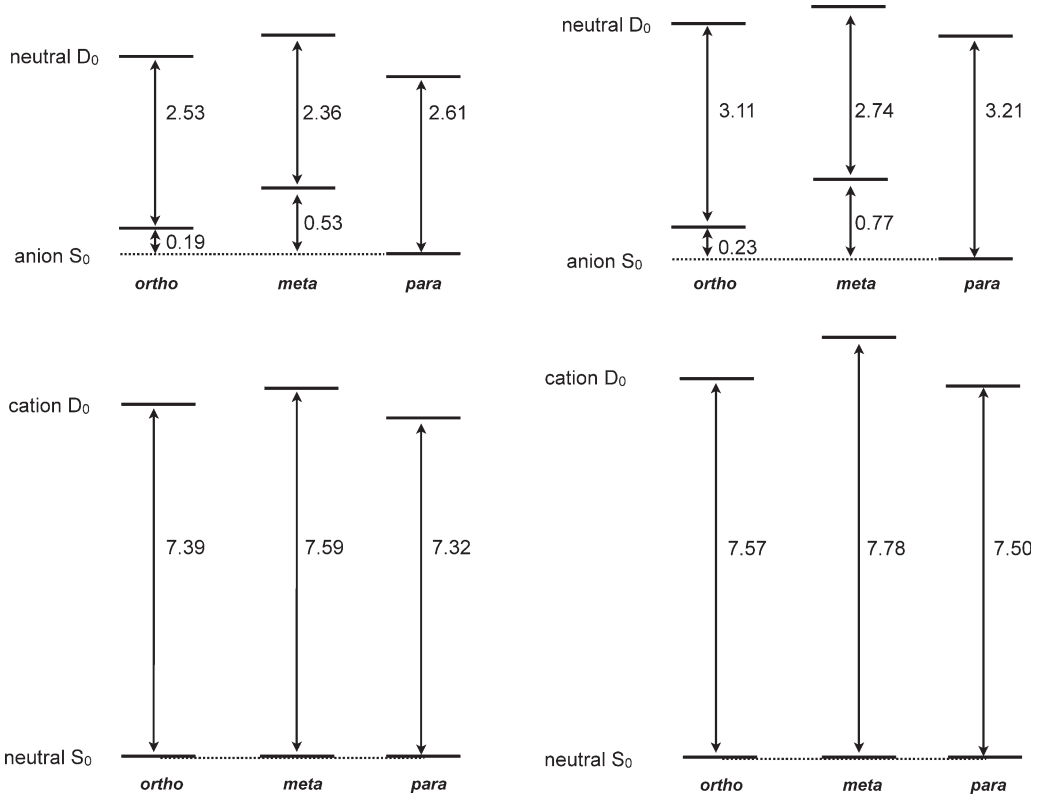

Figure 3. ωB97X-D/cc-pVTZ//RI-MP2/cc-pVTZ vertical ionization and detachment energies, eV, for HBDI (left) and HBMPDI (right) species.

To conclude, the observed trends suggest that the acylimine tail participates in the overall conjugation and enhances its effect; the main differences between the para, meta, and ortho species are similar in the HBDI and HBMPDI series.

Vertical ionization and detachment energies

Computed VIEs are given in Figure 3 and Table 2. The two main factors that determine the differences in IEs/DEs between the green and red chromophores are the resonance and the electronegativity of the acylimine group; we will analyze these two effects in detail. The resonance stabilization is more pronounced in the anionic and cationic (ortho and para) species than in the neutrals and anionic meta forms. Thus, one can expect the following trends in IEs: (i) lower IE for the meta anionic chromophores relative to the para and ortho ones and (ii) greater IE for the meta neutral chromophores compared to the ortho and para forms.[16] The same arguments can be applied to explain IEs/DEs of the green and red chromophores, as the addition of the acylimine bond increases the conjugation lengths and provides additional stabilization of the charged species. However, acylimine is an electronegative group that increases IE. Thus, in the neutrals, resonance stabilization and electronegativity act in the opposite directions, whereas in the anionic chromophores the two effects are synergistic. One can anticipate the strongest effect for the anionic para and ortho species. Below we discuss the aforementioned factors by considering computed VIE/VDEs.

The effects of charge (anionic and neutral forms) and the hydroxyl position on the ground state energies and VIE/VDEs provide insight into the degree of resonance stabilization within the chromophore. In the neutral species, the ground-state energy differences between the ortho, meta, and para isomers are small (less than 0.05 eV), whereas energies of the ionized states show large variations. The para isomers of both HBDI and HBMPDI have the lowest IEs, whereas IEs of the meta isomers are about 0.3 eV higher. The ortho isomers have only slightly higher IEs than para (0.07 eV). These trends suggest that while resonance conjugation is not significant in the neutral species, it becomes much more noticeable in the target charged states where it facilitates the delocalization of the hole and the unpaired spin. The anions, conversely, show large variations in the ground state energies, with the meta isomers 0.5–0.8 eV higher in energy than para, and the ortho isomers 0.2 eV higher than para. More efficient resonance

Table 2. Comparison of VIEs computed as the energy difference between closed-shell and electron-detached states and Koopmans' estimates ($-\varepsilon_{HOMO}$) for various isomers and protonation states of HBDI and HBMPDI. All values are in eV.

System	VIE(ωB97X-D)	$-\varepsilon_{HOMO}$(HF)	$-\varepsilon_{HOMO}$(ωB97X-D)
p-HBDI	7.32	7.51	7.40
m-HBDI	7.59	7.81	7.70
o-HBDI	7.39	7.62	7.48
p-HBDI-D	2.61	2.78	2.78
m-HBDI-D	2.36	2.64	2.72
o-HBDI-D	2.53	2.78	2.53
p-HBMPDI	7.50	7.76	7.65
m-HBMPDI	7.78	8.08	7.95
o-HBMPDI	7.57	7.86	7.73
p-HBMPDI-D	3.21	3.40	3.46
m-HBMPDI-D	2.74	3.10	3.02
o-HBMPDI-D	3.11	3.37	3.40

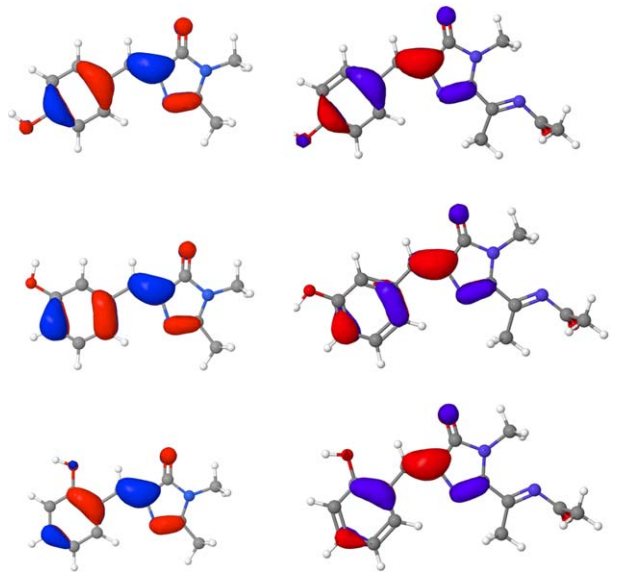

Figure 4. HOMOs of the neutral HBDI and HBMPDI isomers (HF/cc-pVTZ). The isosurface value is 0.05.

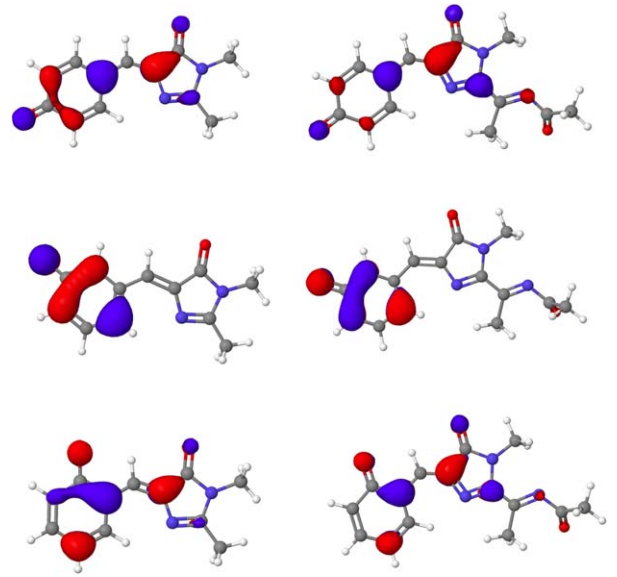

Figure 5. HOMOs of the anionic HBDI and HBMPDI isomers (HF/cc-pVTZ). The isosurface value is 0.05.

delocalization of the negative charge in anions can explain this observation.

Computed VDEs for anionic species are in a reasonable agreement with the reported experimental values of 2.72–2.85 eV.[5–7] However, computed VDEs should not be directly compared with the maximum of the photodetachment band.[19] As shown in Ref. [19], increasing the basis set from cc-pVTZ (used here) to aug-cc-pVTZ can cause a shift of almost 0.2 eV in VDE, resulting in even better agreement with the experiment. Smaller VDE for m-HBDI-D relative to p-HBDI-D is consistent with the experimental results (2.40–2.54 $\pm$ 0.1 eV), as well as previous theoretical studies.[9,16]

Interestingly, the differences between the isomers are larger in HBMPDI than in HBDI. The acylimine fragment enhances charge delocalization, thereby further stabilizing the anion for the para and ortho isomers. In HBDI and HBMPDI, the differences in VDEs between para and meta forms are 0.25 and 0.47 eV, respectively. Thus, the acylimine tail does not mitigate the conjugation effects; rather, it enhances them. Furthermore, the electronegativity of the acylimine fragment causes an increase in the vertical IEs/DEs in all forms of HBMPDI relative to HBDI. As anticipated, the para and ortho anions show the strongest stabilizing effects from the acylimine group because both resonance stabilization and electronegativity contribute to the blue shift of VDE.

We also analyzed the effect of specific position of the OH group on IEs: 2- and 6- for ortho- and 3- and 5- for meta-HBDI-D (Table SI, SI). We found no effect of the substituent position in meta forms; the differences are within 0.04 eV. Greater shifts in IEs were observed for ortho isomers. IE of the 6-o-HBDI-D is 0.14 eV lower than that of 2-o-HBDI-D. The shift can be attributed to the nonplanar geometry of the 6-o-HBDI-D caused by a steric repulsion between the OH group and the nitrogen of the imidazolinone ring. This nonplanarity partially disrupts the conjugation between the rings leading to a red-shifted IE.

Charge and spin densities distributions

To obtain additional insight into the resonance effects on the electronic structure of the ionized states and IEs/DEs, we analyzed the charge and unpaired spin density distributions, as well as the shapes of the HOMOs. The HF canonical HOMOs are shown in Figures 4 and 5. We note that the shapes of the ωB97X-D HOMOs are almost identical to HF ones (see SI)—no overdelocalization is observed. Tables 3 and 4 show the NBO charges and spin densities computed for the phenolate, bridge, imidazolinone, and acylimine moieties.

Table 3. Comparison of partial charges (*Q*) and spin densities (SD) of different moieties of the chromophores in the neutral (N) state and upon the removal of an electron giving rise to radical cation (RC).

System	Quantity	P	B	I	AI
p-HBDI	*Q*, N	0.019	0.128	−0.147	–
	Q, RC	0.581	0.146	0.273	–
	ΔQ	0.562	0.018	0.420	–
	SD, RC	0.578	−0.164	0.586	–
o-HBDI	*Q*, N	0.026	0.131	−0.157	–
	Q, RC	0.480	0.193	0.327	–
	ΔQ	0.454	0.062	0.484	–
	SD, RC	0.431	0.041	0.528	–
m-HBDI	*Q*, N	0.026	0.110	−0.136	–
	Q, RC	0.477	0.182	0.341	–
	ΔQ	0.451	0.072	0.4773	–
	SD, RC	0.432	0.063	0.505	–
p-HBMPDI	*Q*, N	0.070	0.149	−0.226	0.007
	Q, RC	0.539	0.174	0.190	0.096
	ΔQ	0.469	0.025	0.416	0.090
	SD, RC	0.464	−0.011	0.526	0.022
o-HBMPDI	*Q*, N	0.044	0.159	−0.211	0.009
	Q, RC	0.479	0.207	0.215	0.099
	ΔQ	0.434	0.049	0.426	0.091
	SD, RC	0.416	0.028	0.535	0.022
m-HBMPDI	*Q*, N	0.038	0.141	−0.192	0.012
	Q, RC	0.446	0.213	0.238	0.105
	ΔQ	0.407	0.072	0.429	0.092
	SD, RC	0.384	0.068	0.528	0.021

Table 4. Comparison of partial charges (*Q*) and spin densities (SD) of different moieties of the chromophores in the anionic (D) state and upon removal of an electron giving rise to a neutral radical (NR)

System	Quantity	P	B	I	AI
p-HBDI	*Q*, D	−0.624	0.146	−0.522	–
	Q, NR	−0.023	0.780	−0.057	–
	Δ*Q*	0.601	−0.066	0.465	–
	SD, NR	0.710	−0.230	0.520	–
o-HBDI	*Q*, D	−0.705	0.195	−0.490	–
	Q, NR	−0.052	0.117	−0.066	–
	Δ*Q*	0.653	−0.078	0.424	–
	SD, NR	0.762	−0.215	0.453	–
m-HBDI	*Q*, D	−0.833	0.184	−0.351	–
	Q, NR	0.012	0.114	−0.126	–
	Δ*Q*	0.844	−0.070	0.225	–
	SD, NR	1.030	0.028	−0.059	–
p-HBMPDI	*Q*, D	−0.494	0.154	−0.516	−0.144
	Q, NR	0.002	0.088	−0.097	0.007
	Δ*Q*	0.496	−0.065	0.419	0.151
	SD, NR	0.607	−0.228	0.564	0.057
o-HBMPDI	*Q*, D	−0.582	0.211	−0.493	−0.136
	Q, NR	−0.040	0.136	−0.103	−0.006
	Δ*Q*	0.542	−0.074	0.390	0.142
	SD, NR	0.669	−0.221	0.504	0.049
m-HBMPDI	*Q*, D	−0.790	0.217	−0.376	−0.051
	Q, NR	0.029	0.143	−0.187	0.015
	Δ*Q*	0.818	−0.074	0.188	0.067
	SD, NR	1.034	0.028	−0.058	−0.004

As discussed above, the HOMO shape represents the HF unrelaxed Dyson orbital that is related to experimental observables such as cross sections and angular distributions. Dyson orbitals, however, only represent the shape of the hole in the ionized state at the instance of ionization; that is, they do not account for electronic relaxation. Thus, even when using exact wave functions for the initial and target states at the same nuclear geometries (i.e., vertical values), one should anticipate differences between Dyson orbital densities and charge/spin delocalization patterns. Our previous EOM-IP-CCSD calculations of HBDI-D[19] show that the target ionized state is dominated by a single ionized configuration corresponding to electron detachment from the HOMO. Thus, we expect that the HF HOMO is a good approximation to the correlated Dyson orbital in HBDI-D and similar systems.

The shapes of MOs of all neutral species show almost identical delocalization patterns in the ortho, meta, and para isomers. Most of the density resides on phenolate and imidazolinone, and the electronic density on the bridge indicates a double C_BC_I bond. This observation is consistent with the relative ground-state energies of the neutral species (discussed above) that are not significantly altered by the addition of acylimine. Furthermore, spin density in the corresponding ionized forms is also delocalized between the phenolate and imidazolinone (Table 3). In HBDI, the delocalization is almost equal. This pattern is consistent with the shape of the HOMO, which is essentially the same for para, meta, and ortho HBDI. In HBMPDI, the distribution is slightly more asymmetric favoring imidazolinone. Indeed, both partial charge and unpaired spin density on the phenolate ring are smaller for HBMPDI than for HBDI, for example, 0.58 (*Q*, RC) versus 0.54 (*Q*, RC), and 0.578 (SD, RC) versus 0.464 (SD, RC) for p-HBDI and p-HBMPDI. The bridge hosts very little spin density, except in p-HBDI. The spin density and charge density show the same pattern in radical cations.

In the anions, the shape of the HOMO is different and shows larger variations, and the OH group position has a strong effect on the charge and spin density distribution. In para and ortho species, the HOMO has allylic character on the bridge and is delocalized on phenolate and imidazolinone. Para and ortho HBMPDI-D have only minor contributions from the acylimine moiety, although the overall shape suggests stronger delocalization toward imidazolinone than is observed for the HBDI-D analogues. In meta, the HOMO is almost entirely localized on the phenolate; the m-HBMPDI-D species has no electron density on the acylimine. Indeed, for meta isomers the negative charge is predominantly located on the phenolate ring, and the phenolate partial charges are 0.83 and 0.79 for HBDI-D and HBMPDI-D, respectively. In para and ortho HBMPDI-D, the charge is more delocalized, illustrating strong resonance stabilization effect in the ground states of these isomers. Furthermore, the spin density distributions for the neutral radicals are close to the charge changes on the corresponding moiety on ionization (Δ*Q*, Table 4). Consistently with the shape of the HOMOs, both m-HBDI-D and m-HBMPDI-D have a partial spin density of 1.03 on the phenolate ring, indicating that the unpaired electron also resides on the phenolate moiety in the target detached state. Para and ortho forms, conversely, have more extensive delocalization of the unpaired spin, with spin densities between 0.6 and 0.8 on the phenolate fragment.

In sum, acylimine's electronegativity results in greater IEs/DEs for all HBMPDI chromophores relative to their HBDI analogues. The shifts are different for different forms. The largest blue shift is observed in the anionic ortho and para species owing to acylimine bridge participation in the negative charge delocalization and electronegativity of the acylimine moiety acting in synergy (Table 4).

Conclusion

We performed electronic structure studies of the role of resonance delocalization and the extent of the π-system in determining electron-donating ability of model FP chromophores. We quantified and analyzed the effects of ortho, meta, and para position of the OH group in model green (HBDI) and red (HBMPDI) chromophores. To understand the trends in IEs/DEs, we analyzed the structural differences, as well as charge and unpaired spin distribution patterns. The results illustrate that the resonance delocalization affects the structures and energetics of the chromophores. The effect is most pronounced in the anionic species and is stronger for the HBMPDI-D chromophores than for the HBDI-D ones, for example, the ground state of the anionic meta isomer of HBMDPI lies 0.8 eV above the corresponding para form. The cations are also susceptible to resonance stabilization, although the energy differences (at the geometries of the neutrals) are less than in the anions. For example, the energy of the m-HBMPDI radical cation is ∼0.3 eV greater than the energy of the para form. The trends in

IEs/DEs of HBDI and HBMPDI are driven by the resonance stabilization of charged species. As a result, IEs follow the trend para $\approx$ ortho $<$meta and DEs display an opposite ordering, with para $\approx$ ortho $>$meta. The main effect of the acylimine group on the IEs/DEs is due to its electronegativity, which leads to a significant increase in IEs and DEs in all forms of HBMPDI relative to HBDI. Acylimine participation in the resonance delocalization is less significant; it is manifested by greater energy differences between the meta and ortho/para isomers of the anionic HBMPDI species relative to HBDI. Charge and spin density distributions, as well as the shapes of MOs, are consistent with the above analysis. Charge and unpaired spin delocalization patterns are generally consistent with the shapes of the HOMOs, indicating that the relaxation effects are relatively small. Overall, our results reveal that relatively small modifications of the chromophores can cause significant changes in key properties such as electron-donating ability. These insights might be useful to future efforts in bioimaging and FP engineering.

Keywords: biochromophores · ionization · electron detachment · fluorescent proteins · DFT

How to cite this article: J. Lazzari-Dean, A. I. Krylov, K. B. Bravaya. *Int. J. Quantum Chem.* **2014**, *115*, 1258–1264. DOI: 10.1002/qua.24825

Additional Supporting Information may be found in the online version of this article.

[1] M. Y. Okamura, M. L. Paddock, M. S. Graige, G. Feher, *Biochim. Biophys. Acta* **2000**, *1458,* 148.
[2] M. R. Wasielewski, *Chem. Rev.* **1992**, *92*, 435.
[3] S. Weber, *Biochim. Biophys. Acta* **2005**, *1707*, 1.
[4] A. M. Bogdanov, A. S. Mishin, I. V. Yampolsky, V. V. Belousov, D. M. Chudakov, F. V. Subach, V. V. Verkhusha, S. Lukyanov, K. A. Lukyanov, *Nat. Chem. Biol.* **2009**, *5*, 459.
[5] D. A. Horke, J. R. R. Verlet, *Phys. Chem. Chem. Phys.* **2012**, *14*, 8511.
[6] Y. Toker, D. B. Rahbek, B. Klærke, A. V. Bochenkova, L. H. Andersen, *Phys. Rev. Lett.* **2012**, *109*, 128101.
[7] C. R. S. Mooney, M. E. Sanz, A. R. McKay, R. J. Fitzmaurice, A. E. Aliev, S. Caddick, H. H. Fielding, *J. Phys. Chem. A* **2012**, *116*, 7943.
[8] C. R. S. Mooney, M. A. Parkes, L. Zhang, H. C. Hailes, A. Simperler, M. J. Bearpark, H. H. Fielding, *J. Chem. Phys.* **2014**, *140*, 205103.
[9] A. V. Bochenkova, B. Klærke, D. B. Rahbek, J. Rajput, Y. Toker, L. H. Andersen, *Angew. Chem. Int. Ed. Engl.* **2014**, *53*, 9797.
[10] R. Y. Tsien, *Annu. Rev. Biochem.* **1998**, *67*, 509.
[11] F. V. Subach, V. V. Verkhusha, *Chem. Rev.* **2012**, *112*, 4308.
[12] A. J. Meyer, T. P. Dick, *Antioxid. Redox Signal.* **2010**, *13*, 621.
[13] K. A. Lukyanov, V. V. Belousov, *Biochim. Biophys. Acta* **2014**, *1840*, 745.
[14] E. Epifanovsky, I. Polyakov, B. L. Grigorenko, A. V. Nemukhin, A. I. Krylov, *J. Chem. Theory Comput.* **2009**, *5*, 1895.
[15] E. Epifanovsky, I. Polyakov, B. L. Grigorenko, A. V. Nemukhin, A. I. Krylov, *J. Chem. Phys.* **2010**, *132*, 115104.
[16] K. M. Solntsev, D. Ghosh, A. Amador, M. Josowicz, A. I. Krylov, *J. Phys. Chem. Lett.* **2011**, *2*, 2593.
[17] D. Ghosh, A. Acharya, S. C. Tiwari, A. I. Krylov, *J. Phys. Chem. B* **2012**, *116*, 12398.
[18] B. L. Grigorenko, A. V. Nemukhin, D. I. Morozov, I. Polyakov, K. B. Bravaya, A. I. Krylov, *J. Chem. Theory Comput.* **2012**, *8*, 1912.
[19] K. B. Bravaya, A. I. Krylov, *J. Phys. Chem. A* **2013**, *117*, 2293.
[20] R. B. Vegh, K. B. Bravaya, D. A. Bloch, A. S. Bommarius, L. M. Tolbert, M. Verkhovsky, A. I. Krylov, K. M. Solntsev, *J. Phys. Chem. B* **2014**, *118*, 4527.
[21] K. Bravaya, B. L. Grigorenko, A. V. Nemukhin, A. I. Krylov, *Acc. Chem. Res.* **2012**, *45*, 265.
[22] C. M. Oana, A. I. Krylov, *J. Chem. Phys.* **2007**, *127*, 234106.
[23] C. M. Oana, A. I. Krylov, *J. Chem. Phys.* **2009**, *131*, 124114.
[24] J.-D. Chai, M. Head-Gordon, *J. Chem. Phys.* **2008**, *128*, 084106.
[25] J.-D. Chai, M. Head-Gordon, *Phys. Chem. Chem. Phys.* **2008**, *10*, 6615.
[26] T. H. Dunning, *J. Chem. Phys.* **1989**, *90*, 1007.
[27] F. Weigend, M. Häser, H. Patzelt, R. Ahlrichs, *Chem. Phys. Lett.* **1998**, *294*, 143.
[28] E.D. Glendening, J. K. Badenhoop, A. E. Reed, J. E. Carpenter, F. Weinhold, NBO 4.0. Theoretical Chemistry Institute; University of Wisconsin: Madison, WI, **1996**.
[29] K. B. Bravaya, E. Epifanovsky, A. I. Krylov, *J. Phys. Chem. Lett.* **2012**, *3*, 2726.
[30] A. I. Krylov, P. M. W. Gill, *Wiley Interdiscip. Rev. Comput. Mol. Sci.* **2013**, *3*, 317.
[31] Y. Shao, Z. Gan, E. Epifanovsky, A. T. B. Gilbert, M. Wormit, J. Kussmann, A. W. Lange, A. Behn, J. Deng, X. Feng, D. Ghosh, M. Goldey, P. R. Horn, L. D. Jacobson, I. Kaliman, R. Z. Khaliullin, T. Kus, A. Landau, J. Liu, E. I. Proynov, Y. M. Rhee, R. M. Richard, M. A. Rohrdanz, R. P. Steele, E. J. Sundstrom, H. L. Woodcock, III, P. M. Zimmerman, D. Zuev, B. Albrecht, E. Alguires, B. Austin, G. J. O. Beran, Y. A. Bernard, E. Berquist, K. Brandhorst, K. B. Bravaya, S. T. Brown, D. Casanova, C.-M. Chang, Y. Chen, S. H. Chien, K. D. Closser, D. L. Crittenden, M. Diedenhofen, R. A. DiStasio, Jr., H. Do, A. D. Dutoi, R. G. Edgar, S. Fatehi, L. Fusti-Molnar, A. Ghysels, A. Golubeva-Zadorozhnaya, J. Gomes, M. W. D. Hanson-Heine, P. H. P. Harbach, A. W. Hauser, E. G. Hohenstein, Z. C. Holden, T.-C. Jagau, H. Ji, B. Kaduk, K. Khistyaev, J. Kim, J. Kim, R. A. King, P. Klunzinger, D. Kosenkov, T. Kowalczyk, C. M. Krauter, K. U. Laog, A. Laurent, K. V. Lawler, S. V. Levchenko, C. Y. Lin, F. Liu, E. Livshits, R. C. Lochan, A. Luenser, P. Manohar, S.F. Manzer, S.-P. Mao, N. Mardirossian, A.V. Marenich, S.A. Maurer, N.J. Mayhall, C. M. Oana, R. Olivares-Amaya, D. P. O'Neill, J. A. Parkhill, T. M. Perrine, R. Peverati, P. A. Pieniazek, A. Prociuk, D. R. Rehn, E. Rosta, N. J. Russ, N. Sergueev, S. M. Sharada, S. Sharmaa, D. W. Small, A. Sodt, T. Stein, D. Stuck, Y.-C. Su, A. J. W. Thom, T. Tsuchimochi, L. Vogt, O. Vydrov, T. Wang, M. A. Watson, J. Wenzel, A. White, C. F. Williams, V. Vanovschi, S. Yeganeh, S. R. Yost, Z.-Q. You, I. Y. Zhang, X. Zhang, Y. Zhou, B.R. Brooks, G.K.L. Chan, D.M. Chipman, C.J. Cramer, W.A. Goddard III, M.S. Gordon, W. J. Hehre, A. Klamt, H. F. Schaefer, III, M.W. Schmidt, C. D. Sherrill, D. G. Truhlar, A. Warshel, X. Xu, A. Aspuru-Guzik, R. Baer, A. T. Bell, N. A. Besley, J.-D. Chai, A. Dreuw, B. D. Dunietz, T. R. Furlani, S. R. Gwaltney, C.-P. Hsu, Y. Jung, J. Kong, D. S. Lambrecht, W. Z. Liang, C. Ochsenfeld, V. A. Rassolov, L.V. Slipchenko, J. E. Subotnik, T. Van Voorhis, J. M. Herbert, A. I. Krylov, P. M. W. Gill, M. Head-Gordon, *Mol. Phys.* (in press). Doi: doi: 10.1080/00268976.2014.952696.

Received: 6 August 2014
Revised: 3 November 2014
Accepted: 6 November 2014
Published online 2 December 2014